Nanometer-Scale Smectic Ordering of Genetically Engineered Rodlike Polymers: Synthesis and Characterization of Monodisperse Derivatives of Poly(γ-benzyl α,L-glutamate)

Seungju M. Yu,[†,⊥] Carissa M. Soto,[‡] and David A. Tirrell*[,†,§]

Contribution from the Department of Polymer Science and Engineering, and Department of Chemistry, University of Massachusetts, Amherst, Massachusetts 01003, and Division of Chemistry and Chemical Engineering, California Institute of Technology, Pasadena, California 91125

Received February 7, 2000

Abstract: Macromolecules with precisely defined architectures on the nanometer scale are ideal building blocks for self-assembled materials and nanometer-scale devices. By utilizing recombinant DNA technology and bacterial protein expression, we have prepared a set of rodlike artificial proteins, Glu(OBzl)Asp(OBzl)[Glu-(OBzl)$_{17}$Asp(OBzl)]$_X$-Glu(OBzl)Glu(OBzl) (PBLG-*X*, $X = 3-6$, **1**), which serve as monodisperse analogues of poly(γ-benzyl α,L-glutamate) (PBLG), with variation of rod length from 8.7 to 17 nm. Synthesis was accomplished by (i) bacterial production of a precursor polypeptide GluAsp(Glu$_{17}$Asp)$_X$GluGlu (PLGA-*X*, $X = 3-6$), as a fusion to mouse dihydrofolate reductase (DHFR), (ii) CNBr digestion of the expressed protein to liberate PLGA-*X*, and (iii) side chain benzylation of PLGA-*X* via treatment with phenyldiazomethane. The growth rates of cultures transformed with the recombinant genes, and the yields of protein expressed therein, depended on the number of Glu$_{17}$Asp repeats appended to the fusion partner, decreasing as the number of repeats increased. PBLG-3, with the lowest aspect ratio (6.9), did not exhibit liquid crystalline (LC) behavior while each of the other polymers formed lyotropic LC phases. The phase transition behavior of PBLG-*X* was distinctly different from that of conventional polydisperse PBLG; when the concentration of the polymer solution was gradually increased, the transition from the isotropic to the liquid crystalline state occurred uniformly throughout the sample without formation of distinct birefringent droplets. Solution-cast films of PBLG-4 and PBLG-5 formed smectic supramolecular architectures with layer spacings (11.4 and 14.0 nm, respectively) precisely determined by the length of the monodisperse rods. Smectic ordering was observed only in films cast from mixtures of chloroform (97%) and trifluoroacetic acid (3%). In films prepared from dioxane, both polydisperse and monodisperse PBLGs adopted columnar order without formation of smectic layers.

Introduction

Research on self-assembling materials is an exciting and active scientific discipline that may lead to a variety of novel nanometer-scale devices.[1,2] The key feature of the self-assembly process is the development of supramolecular order via noncovalent interactions, and because assembly occurs spontaneously, the design of the requisite building blocks constitutes the most critical step in controlling material properties. Macromolecules with architectures precisely defined at the nanometer scale are considered to be ideal as elements of nanostructured materials; however, only a few well-defined synthetic building blocks of nanometer size are available.[3−5] Macromolecular assemblies of precisely defined architecture are difficult to achieve with synthetic polymers since inhomogeneity in both sequence and molecular weight works against the formation of well-defined supramolecular arrangements.

As an alternative to chemical polymerization processes, the synthesis, cloning, and expression of artificial DNA has provided a powerful tool for the preparation of structurally homogeneous "artificial proteins".[6,7] Utilization of this technique has allowed preparation of nonnatural polypeptide sequences with near-absolute control of size, composition, sequence, and stereochemistry.[8,9] Furthermore, the gene of interest can be designed to control not only the molecular but also the supramolecular architecture of the target artificial protein, in a process which might be described as "encoded self-assembly". In this article we discuss a particularly interesting class of artificial proteins, monodisperse derivatives of poly(γ-benzyl α,L-glutamate) (PBLG), which are characterized by rodlike molecular structure, and which can self-assemble to form layered structures with fine control on the nanometer length scale.

[†] Department of Polymer Science and Engineering, University of Massachusetts at Amherst.
[‡] Department of Chemistry, University of Massachusetts at Amherst.
[§] California Institute of Technology.
[⊥] Current address: Department of Chemistry, University of Wisconsin, Madison, WI 53706.

(1) Philp, D.; Stoddart, J. F. *Angew. Chem., Int. Ed. Engl.* **1996**, *35*, 1154.
(2) Timp, G. *Nanotechnology*; AIP Press: New York, 1999.
(3) Andres, R. P.; Bielefeld, J. D.; Henderson, J. I.; Janes, D. B.; Kolagunta, V. R.; Kubiak, C. P.; Mahoney, W. J.; Osifchin, R. G. *Science* **1996**, *273*, 1690.
(4) Kriesel, J. W.; Konig, S.; Freitas, M. A.; Marshall, A. G.; Leary, J. A.; Tilley, T. D. *J. Am. Chem. Soc.* **1998**, *120*, 12207.
(5) Murray, C. B.; Kagan, C. R.; Bawendi, M. G. *Science* **1995**, *270*, 1335.
(6) Cappello, J.; Crissman, J.; Dorman, M.; Mikolajczak, M.; Textor, G.; Marquet, M.; Ferrari, F. *Biotechnol. Prog.* **1990**, *6*, 198.
(7) McGrath, K. P.; Tirrell, D. A.; Kawai, M.; Mason, T. L.; Fournier, M. J. *Biotechnol. Prog.* **1990**, *6*, 188.
(8) Krejchi, M. T.; Atkins, E. D. T.; Waddon, A. J.; Fournier, M. J.; Mason, T. L.; Tirrell, D. A. *Science* **1994**, *265*, 1427.
(9) Petka, W. A.; Harden, J. L.; McGrath, K. P.; Wirtz, D.; Tirrell, D. A. *Science* **1998**, *281*, 389.

10.1021/ja000465p CCC: $19.00
Published on Web 06/29/2000

PBLG is a typical helical polypeptide with a stiff "rigid-rod" structure. Because of its ready availability and good solubility combined with its well-behaved rodlike structure, PBLG has been extensively studied with respect to its helix-coil transition and its dielectric, hydrodynamic, and liquid crystalline (LC) properties.[10] In addition, the interfacial behavior of PBLG and its derivatives has recently drawn attention, owing to opportunities for engineering functional surface arrays.[11−15] Interpretation of the physical properties of PBLG and the preparation of highly ordered supramolecular architectures are complicated by the polydispersity of PBLGs prepared by ring-opening polymerization of the *N*-carboxy-α-amino acid anhydride.[16,17]

Since their discovery by Robinson, the lyotropic liquid crystalline phases (cholesteric and nematic) exhibited by PBLG have served as important model systems for rod-ordering theories of the liquid crystalline state.[18,19] Phase diagrams of PBLG solutions have been determined experimentally[20,21] and are in general agreement with those predicted by Flory;[22] however, critical comparison of theory and experiment has been complicated by the polydispersity of conventional PBLG. One of the questions that has puzzled investigators for many years is the absence of smectic phases in lyotropic PBLG systems. Smectic ordering is common in low molecular weight LC compounds and there is no obvious reason similar order should be precluded in rodlike polymers. Tobacco mosaic virus, a monodisperse rodlike protein assembly, forms smectic phases in colloidal solutions.[23] Layered supramolecular structures of wormlike polymers[24] or rod-coil block copolymers[25] have also been reported recently; however, no direct evidence for smectic order in conventional PBLG is available to date.

We have recently reported preparation of a monodisperse derivative of PBLG via recombinant DNA technology, and presented evidence for smectic order in solutions and films of the polymer.[26] In the absence of an aligning field, the chirality of the rods imposes a twist on the smectic order and a twist grain boundary-like morphology is observed.[27] In this article, we present detailed synthetic techniques for preparation of a series of monodisperse nanometer-size, rodlike derivatives of PBLG (PBLG-*X*, **1**). The number of octadecameric repeating units (*X*) was varied from 3 to 6, corresponding to variation of the α-helical rod length from 8.7 to 17 nm. The goal of this work was to explore the prospects for engineering of nanometer-scale smectic layer spacings in systems of molecular rods. We present here the liquid crystalline properties of monodisperse, rodlike artificial proteins, with special attention to smectic ordering in solutions and in films. Our results show that, within limits, smectic layer spacings can be controlled precisely by the length of the constituent macromolecular rods.

$$\mathrm{Glu(OBzl)Asp(OBzl)[Glu(OBzl)_{17}Asp(OBzl)]_X\text{-}Glu(OBzl)Glu(OBzl)}$$

1: PBLG-*X* (*X* = 3−6)

Experimental Section

Materials. T4 DNA ligase, calf intestinal phosphatase (CIP), and all restriction enzymes were purchased from New England Biolabs (Beverly, MA). Ribonuclease A, deoxyribonuclease I, antifoam agent, ampicillin, kanamycin, cyanogen bromide, phenylmethylsulfonyl fluoride (PMSF), polydisperse PLGA (DP ≈ 98, PDI = 1.2), and PBLG (DP ≈ 98, PDI = 1.2) were purchased from Sigma Chemical Co. *Escherichia coli* strain DH5αF′ and plasmid pUC18 were purchased from Bethesda Research Laboratories (Bethesda, MD). DEAE Sephadex A-25 anion-exchange resin and ECL western blotting detection reagents were purchased from Amersham-Pharmacia Biotech Inc (NJ). Expression plasmid pQE15, *E. coli* strain SG13009 containing pREP4, and Ni-nitrilo-triacetic acid (Ni-NTA) resin were purchased from Qiagen Inc (Chatsworth, CA). HPLC grade benzene, trifluoroacetic acid, and dimethyl sulfoxide (HPLC grade) were purchased from Aldrich Chemical Co. All materials were used without further purification.

General Methods. Procedures for DNA manipulation, transformation, bacterial growth, gel electrophoresis, and western blot analysis were adopted from published literature or from instructions provided by manufacturers.[28] Large scale fermentations were run in a New Brunswick 80 L mobile pilot plant (MPP-80); cells were harvested in a Cepa Z41 continuous centrifuge. Ultrafiltration was performed in Centriprep concentrators (molecular weight cut off 3000) purchased from Amicon Inc. Amino acid composition analyses were obtained from the Molecular and Cell Biology Core Facility at the University of Massachusetts at Amherst. Matrix-assisted laser desorption/ionization (MALDI) time-of flight (TOF) mass spectra were recorded on a Bruker Reflex II instrument. X-ray diffraction patterns were recorded with pinhole collimation and Ni-filtered Cu Kα radiation in either an evacuated flat-plate Rigaku small-angle X-ray camera or a flat-plate Statton Camera. The beam direction was normal to the film surface. Polarized light optical micrographs were taken on an Olympus BX microscope at room temperature.

Preparation of Monomeric DNA. Plasmid pUC18-89 (pUC18 carrying *Bam*HI insert **2**) was isolated from transformed *E. coli* strain DH5αF′ cells as described.[29] The isolated plasmid was digested with *Bbs*I and the resulting *Bbs*I fragment ("monomeric" DNA) was purified on a 15% polyacrylamide gel.

Generation of Multimers. The monomer (*Bbs*I fragment of pUC18-89) solution (3 μL, 10 ng/μL) from above was mixed with 1 μL of 10 × ligation buffer and 5.5 μL of H_2O. T4 DNA ligase (0.5 μL, 20 units/μL) was added and the reaction mixture was incubated at 14 °C. After 24 h, a linearized pUC18-89 without the 54 bp *Bbs*I fragment (4 μL, 2.5 ng/μL) was added and another 0.5 μL of T4 DNA ligase, 1 μL of 10 × ligation buffer, and 4.5 μL of H_2O were added. After 24 h incubation at 14 °C, the ligation mixture was directly used to transform *E. coli* strain DH5αF′ competent cells which were then grown on a 2 × YT medium plate supplemented with 200 mg/mL ampicillin. Plasmids were isolated and digested with *Bam*HI as described before. Transformants containing 3, 4, 5, and 6 repeats of the DNA monomer segment were chosen for further analysis. These recombinant plamids were designated pUC803-*X*, *X* being the number of repeats of the monomeric DNA in the synthetic insert.

(10) Block, H. *Poly(γ-benzyl-L-glutamate) and Other Glutamic Acid Containing Polymers*; Gordon and Breach: New York, 1993.
(11) Chang, Y.-C.; Frank, C. *Langmuir* **1996**, *12*, 5824.
(12) Jaworek, T.; Neher, D.; Wegner, G.; Wieringa, R. H.; Schouten, A. J. *Science* **1998**, *279*, 57.
(13) Whitesell, J. K.; Chang, H. K. *Science* **1993**, *261*, 73.
(14) Enriquez, E. P.; Gray, K. H.; Guarisco, V. F.; Linton, R. W.; Mar, K. D.; Samulski, E. T. *J. Vac. Sci. Technol. A* **1992**, *10*, 2775.
(15) Mathauer, K.; Schmidt, A.; Knoll, W.; Wegner, G. *Macromolecules* **1995**, *28*, 1214.
(16) Kricheldorf, H. R. α-Aminoacid-*N-Carboxy-Anhydrides and Related Heterocycles*; Springer: New York, 1987.
(17) Deming, T. J. *Nature* **1997**, *390*, 386.
(18) Straley, J. P. *Mol. Cryst. Liq. Cryst.* **1973**, *22*, 333.
(19) Robinson, C.; Ward, J. C. *Nature* **1957**, *180*, 1183.
(20) Horton, J. C.; Donald, A. M.; Hill, A. *Nature* **1990**, *346*, 44.
(21) Wee, E. L.; Miller, W. G. *J. Phys. Chem.* **1970**, *75*, 1446.
(22) Flory, P. J. *Proc. R. Soc. London, Ser. A* **1956**, *234*, 73.
(23) Wen, X.; Meyer, R. B.; Caspar, D. L. D. *Phys. Rev. Lett.* **1989**, *63*, 2760.
(24) Albrecht, C.; Lieser, G.; Wegner, G. *Prog. Colloid Polym. Sci.* **1993**, *92*, 111.
(25) Chen, J. T.; Thomas, E. L.; Ober, C. K.; Mao, G.-p. *Science* **1996**, *273*, 343.
(26) Yu, S. M.; Conticello, V. P.; Zhang, G.; Kayser, C.; Fournier, M. J.; Mason, T. L.; Tirrell, D. A. *Nature* **1997**, *389*, 167.
(27) Hye, S.; Lee, C.; Gido, S. P.; Yu, S. M.; Tirrell, D. A. *Macromolecules* **1998**, *31*, 9387.
(28) Sambrook, J.; Fritsch, E. F.; Maniatis, T. *Molecular Cloning: A Laboratory Manual*, 2nd ed.; Spring Harbor Laboratory Press: New York, 1989.
(29) Zhang, G.; Fournier, M. J.; Mason, T. L.; Tirrell, D. A. *Macromolecules* **1992**, *25*, 3601.

Construction of Bacterial Expression Vectors. Plasmids pUC803-3, -4, -5, and -6 were isolated from the transformed *E. coli* strain DH5αF′ as described earlier. The isolated plasmids were digested with *Bam*HI and purified on a 1.5% agarose gel. The purified *Bam*HI fragments were inserted into the *Bgl*II site of expression vector pQE15 and the resulting recombinant plasmid was transformed into *E. coli* strain SG13009 which also carries plasmid pREP4.[30] The presence and orientation of inserts in the recombinant plasmids were determined by digestion of recombinant plasmids with *Ava*I which yields restriction fragments of sizes dependent on the direction of insertion. The recombinant plasmids were designated pQE15-*X* and the recombinant strains as SG13009/pREP4/pQE15-*X*.

Protein Expression. A single colony of *E. coli* strain SG13009/pREP4/pQE15-*X* was used to inoculate 5 mL of 2 × YT medium containing 200 μg/mL of ampicillin and 30 μg/mL of kanamycin. After overnight incubation at 37 °C, this culture was used to inoculate 100 mL of the same medium and cells were grown at 37 °C. When the culture reached $OD_{600} \approx 1.2$, expression of the target protein was induced by addition of β-isopropylthiogalactoside (IPTG) to a final concentration of 0.01 mM. After 3 h, cells were isolated by centrifugation and the protein contents of whole cell lysates were analyzed by 12% SDS-PAGE with coomassie blue staining. For the western blot experiment, proteins were transferred to a nitrocellulose membrane and target protein was analyzed using mouse anti-RGS-$(His)_4$ as described.[31]

Large-Scale Expression and Purification of Fusion Proteins. A single colony of *E. coli* strain SG13009/pREP4/pQE15-*X* was used to inoculate 10 mL of 2 × YT supplemented with ampicillin (200 μg/mL) and kanamycin (30 μg/mL). These cultures were grown to saturation and used to inoculate 1 L of the same medium. An overnight culture of this medium was used to inoculate 60 L of 1 × YT medium containing ampicillin (100 μg/mL), kanamycin (20 μg/mL), and 3 mL of antifoam agent. This culture was incubated at 37 °C with aeration and agitation until $OD_{600} \approx 1.2$. IPTG was added to a final concentration of 0.01 mM to induce target protein synthesis. After 3 h, cells were isolated by continuous centrifugation, resuspended in 1 L of sterile H_2O, and frozen at −80 °C.

Cells were lysed by repeated cycles of thawing and freezing. To the lysate (500 mL) were added 300 mL of sterile water, 60 mL of 5 M NaCl, 15 mL of 1 M Tris-Cl pH 7.9, PMSF (50 mg), and egg white lysozyme (0.1 mg). The mixture was incubated at 37 °C for 2 h. Subsequently, $MgCl_2$ (6 mmol), DNAseI (0.1 mg), and RNAseA (0.1 mg) were added, and the lysate was incubated for another 3 h. The mixture was centrifuged at 18 000 ×g for 50 min at 4 °C. The supernatant was decanted and the pellet was dissolved in 1 L of binding buffer (6 M guanidine chloride, 0.1 M NaH_2PO_4, 0.01 mM Tris-Cl, pH 8.0) and stirred overnight after adjusting the pH to 8.0. The insoluble materials were removed by centrifugation at 39,200 ×g for 50 min at 4 °C. The clear supernatant was mixed with 150 mL of Ni-NTA resin previously equilibrated with the binding buffer and stirred overnight at room temperature. The resin was isolated by centrifugation at 950 ×g for 45 min, combined with 400 mL of binding buffer, and stirred for 4 h. The resin was isolated again by low speed centrifugation (950 ×g) and washed with 400 mL of wash buffer (8 M urea, 0.1 M NaH_2PO_4, 0.01 mM Tris-Cl, pH 8.0) followed by another wash with 700 mL of second wash buffer (8 M urea, 0.1 M NaH_2PO_4, 0.01 mM Tris-Cl, pH 6.9) as described above. The resin mixture was transferred to a column (5.5 × 20 cm) and sequentially washed with 400 mL of first elution buffer (8 M urea, 0.1 M NaH_2PO_4, 0.01 mM Tris-Cl, pH 5.4) and 200 mL of a second elution buffer (8 M urea, 0.1 M NaH_2PO_4, 0.01 mM Tris-Cl, pH 4.5). All washes and the column flow-through were collected as separate fractions. The protein content of each fraction was analyzed by 12% SDS-PAGE. The fraction containing pure product (pH 5.4 elution) was transferred to dialysis tubing (MWCO = 12−14 kD) and dialyzed for 5 days against running distilled water. The dialysate was lyophilized to afford purified fusion protein, designated PLGA-*X*-DHFR (Table 1).

Cyanogen Bromide Cleavage of Fusion Protein. In a typical procedure, the fusion protein (260 mg) was dissolved in 96% formic acid (190 mL) and H_2O was added to adjust the concentration to 70% formic acid. To this solution, 260 mg of cyanogen bromide was added and the clear mixture was purged with N_2 for 15 min. The reaction was protected from light and stirred for 48 h at room temperature. Volatile compounds were removed by rotary evaporation followed by overnight evacuation under dynamic vacuum. The residual solids were resuspended in 50 mM Tris-Cl (pH 8.0, 150 mL) by vigorous stirring for 12 h and the pH was adjusted to 8.0 with dilute aqueous NaOH. After centrifugation, the clear supernatant was used to charge a column of 50 mL of DEAE-Sephadex A-25 previously equilibrated with 50 mM Tris-Cl, pH 8.0. The charged column was sequentially washed with 250 mL volumes of buffer solutions (50 mM Tris-Cl pH 8.0) containing 100 mM, 500 mM, 2 M, and 4 M NaCl, respectively. Each of these washes was collected as separate fractions and individual fractions were analyzed by electrophoresis on a nondenaturing 12% polyacrylamide gel as described below. The cleaved product was located exclusively in the 2 M NaCl fraction. This fraction was transferred to dialysis tubing (MWCO = 2−5 kD) and dialyzed for 5 days against running distilled water. The dialysate was lyophilized to yield pure cleaved protein PLGA-*X* (Table 1). ^{1}H NMR (D_2O, 200 MHz) δ 2.0−2.3 (2H, γ-CH_2), 2.3−2.7 (2H, β-CH_2), 4.0−4.3 (1H, α-CH); MALDI-TOF *m*/*z* calcd for PLGA-3 7446, found 7452, calcd for PLGA-4 9755, found 9765, calcd for PLGA-5 12063, found 12080, calcd for PLGA-6 14372, found 14389; amino acid analyses calcd for PLGA-3 Asp (6.9%), Glu (93.1%), found Asp (8.6%) Glu (80.8%), calcd for PLGA-4 Asp (6.6%), Glu (93.4%), found Asp (6.6%), Glu (93.4%), calcd for PLGA-5 Asp (6.4%), Glu (93.6%), found Asp (6.4%), Glu (93.6%), calcd for PLGA-6 Asp (6.3%), Glu (93.7%), found Asp (6.2%), Glu (93.8%).

Table 1. Yields and Molecular Weights of Purified Proteins from 60 L Expression

	PLGA-3	PLGA-4	PLGA-5	PLGA-6
yield of PLGA-*X*-DHFR[a]	9.3	10	7.2	5.0
yield of PLGA-*X*[b]	1.2	1.3	0.95	0.92
observed MW of PLGA-*X*[c]	7452	9765	12080	14389
calculated MW of PLGA-*X*	7446	9755	12063	14372

[a] In mg/L. After Ni-NTA affinity column purification. [b] In mg/L. After CNBr reaction and anion-exchange chromatography purification. [c] From MALDI-TOF mass spectrometry.

Polyacrylamide Gel Electrophoresis of PLGA-*X*. Approximately 10 μL of each PLGA-*X* and polydisperse PLGA (DP ≈ 98, PDI = 1.2) solutions (1 μg/μL) were loaded on a 12% polyacrylamide gel and subjected to electrophoresis at 25 mA for 3 h in 0.01 M Na_2HPO_4 (pH 8.0). The gel was washed with water for 10 min and stained with 0.1% methylene blue solution (pH 6.5) for 30 min. The target bands were visible after 3−4 h of destaining in distilled water.

Synthesis of PBLG-*X* (1). The following procedure is representative of the method used for benzylation of PLGA-*X*. PLGA-4 (sodium salt, 100 mg, 0.6 mmol repeating unit) was dissolved in 15 mL of water and acidified with dilute aqueous HCl (final pH 1.3). The precipitated polymer was washed with distilled water (5 × 15 mL) by ultrafiltration (Amicon, MWCO = 3 kD) to remove residual NaCl, and dried under vacuum overnight. The polymer was dissolved in 40 mL of dimethyl sulfoxide, and 20 mL of a phenyldiazomethane (1.3 mmol) solution in benzene was added.[26] The reaction mixture was stirred at room temperature for 48 h in the dark and concentrated to dryness by vacuum distillation. The remaining solid was dissolved in 5 mL of dichloromethane and precipitated by addition to 50 mL of pentane. Similar procedures were used for the preparation of PBLG-3, -5, and -6. ^{1}H NMR ($CDCl_3$ containing 30% deuterated trifluoroacetic acid, 200 MHz) δ 2.0−2.1 (2H, β-CH_2), 2.4 (2H, γ-CH_2), 2.9 (benzyl aspartate β-CH_2), 4.6 (1H, α-CH), 4.9 (benzyl aspartate α-CH), 5.1 (2H, benzylic CH_2), 7.3 (5H, Ar−H).

Preparation of Liquid Crystalline Solutions. Solid PBLG (0.5−1 mg) was transferred to a glass capillary tube (2 mm diameter) and $CHCl_3$(97%)/TFA(3%) solvent mixture (2−10 μL) was delivered to the capillary tube with a microsyringe. The capillary tube was cooled with liquid N_2 and carefully flame-sealed. To solubilize the solid PBLG, the capillary tube was placed inside a centrifugation tube containing

(30) Gottesmann, S.; Halpern, E.; Trisler, P. *J. Bacteriol.* **1981**, *148*, 265.

(31) Rosewell, D. F.; White, E. H. *Methods Enzymol.* **1978**, *57*, 409.

water and centrifuged at low speed. This process was repeated, alternating the centrifugation direction until the solution appeared homogeneous. For direct microscopic observation, the capillary was immersed in water to minimize image distortion. In some cases, the solution was transferred to a slide glass by syringe for immediate observation.

Preparation of PBLG Films. Concentrated solutions of PBLG in $CHCl_3$(97%)/TFA(3%) or dioxane were prepared in vials. These solutions (0.3 mL) were placed on a Teflon plate (2 × 3 cm) and annealed for 4 days at room temperature with the same solvent vapor by incubating the sample in a closed vessel containing the solvent. The solvent was slowly evaporated over a period of 2 to 3 days and residual solvent was removed under vacuum for 2 days. The film was carefully removed from the Teflon surface and used directly for polarized-light optical microscopy and X-ray diffraction experiments.

Results and Discussion

Gene Construction. The design, synthesis, and cloning of oligonucleotide **2**, which encodes the repeating unit $Glu_{17}Asp$ of $GluAsp(Glu_{17}Asp)_XGluGlu$ (PLGA-*X*, $X = 3-6$), were reported previously.[29] Because glutamic acid (Glu) is encoded by just two codons, GAA and GAG, incorporation of restriction sites into genes encoding poly(α,L-glutamic acid) would require use of long stretches of a single codon for the remainder of the sequence, a situation that might cause genetic instability. To avoid potential problems of this kind, aspartic acid (Asp) was encoded at intervals of 18 amino acid residues, to provide recognition and cleavage sites for the restriction enzyme *Bbs*I.[29] Because Asp is structurally similar to Glu and because poly(γ-benzyl α,L-aspartate) has been reported as a stable α-helical polypeptide,[32−34] we did not anticipate disruption of the PBLG-*X* helix due to periodic insertion of Asp. The helical conformation of PLGA-4 in acidic solutions and in films has been confirmed by circular dichroism and infrared spectroscopy.[35]

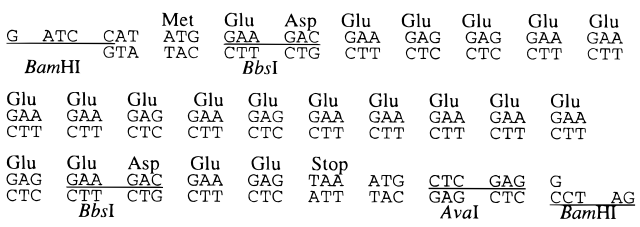

2

Oligonucleotide **2** contains an upstream methionine codon that allows liberation of the target protein, PLGA-*X*, from the N-terminal fusion fragment by cyanogen bromide cleavage, and a stop codon to terminate translation after the last Glu residue. The coding sequences required for preparation of PLGA-*X* were constructed by (i) isolation of the 54 bp *Bbs*I fragment of **2**, (ii) multimerization of the *Bbs*I fragment in head-to-tail fashion, and (iii) insertion of the multimeric DNA into pUC803. Rather than isolating individual multimers after the multimerization step, we inserted a population of chain-length variants into pUC803 and screened for the target lengths after transformation of *E. coli* strain DH5αF′. From an analysis of 66 colonies by *Bam*HI digestion of purified plasmids, transformants containing multimeric DNAs ranging in size from 1 to 10 repeats of the monomer segment were identified (designated as pUC803-*X*, X = number of repeats of monomer segment). The purified *Bam*HI fragments of pUC803-3, -4, -5, and -6 were inserted into the *Bgl*II site of expression vector pQE15. The resulting plasmids were designated pQE15-*X*. The presence and orientation of inserts in the recombinant expression plasmids were confirmed by digestion with *Ava*I, which yields restriction fragments of sizes dependent on the direction of insertion.

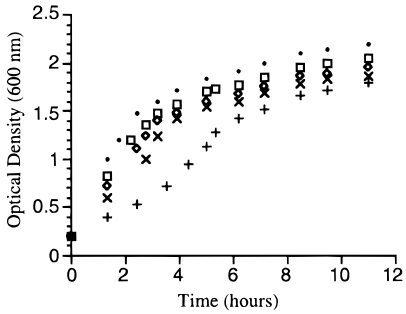

Figure 1. Cell growth profiles of *E. coli* strain SG13009/pREP4 transformed with pQE15 (circles), or with pQE15-*X*, $X = 3$ (squares), 4 (diamonds), 5 (×), and 6 (+). IPTG was added at $OD_{600} = 1.2$ to induce target protein expression.

Protein Expression. Zhang et al. have reported expression of PLGA-4 as a fusion to glutathione *S*-transferase using the pGEX-3X expression vector.[29,36] The proteins of interest in this work were produced from the pQE15 expression system in which the target protein is expressed as a C-terminal fusion to mouse dihydrofolate reductase (DHFR). The fusion proteins also contain six consecutive histidine (His) residues at the N-terminus to allow purification by immobilized metal affinity chromatography.[37] In this expression system, transcription of the target gene is driven by a powerful T5 promoter and is regulated by a double *lac* operator sequence.[38] Figure 1 shows growth profiles of five *E. coli* strains (SG13009/pREP4) transformed with pQE15 or with pQE15-3, -4, -5, and -6, respectively. A gradual reduction of growth rate is evident as the size of the multimeric inserts increases. Reduced growth rates of transformants harboring longer inserts were also evident when cells were grown from single colonies on culture plates; under similar incubation conditions, colonies were much smaller for cells containing longer multimeric inserts. Since the reduced growth rate is observed even before induction, it is unlikely to be a result of toxicity of the expressed protein. Recent work has shown that, under appropriate conditions, large amounts of PLGA-*X* can be accumulated in the bacterial cell, further supporting this argument.[39] It is doubtful that the longer generation time is a consequence of slow replication of the repetitive DNA sequence since the target gene represents a negligible fraction of the cellular DNA. The reduction in growth rate was not observed for *E coli* strain DHαF′ transformed with cloning vector pUC803-*X*. We suggest that the variation in growth rate is caused at the RNA level, and are investigating alternative mechanisms that may account for the growth rate reduction.

SDS-PAGE and western blot analyses of whole cell lysates containing fusion proteins PLGA-*X*-DHFR are shown in Figure 2. New protein bands with apparent molecular weights of 33 400, 35 700, 38 000, and 40 300 can be detected in lanes 2, 3, 4, and 5, respectively. These bands are absent before induction

(32) Riou, S. A.; Hsu, S. L.; Stidham, H. D. *Langmuir* **1998**, *14*, 3062.
(33) Suzuki, Y.; Inoue, Y.; Chujo, R. *Makromol. Chem.* **1980**, *181*, 165.
(34) Tandon, P.; Gupta, V. D.; Prasad, O.; Rastogi, S.; Katti, S. B. *J. Polym. Sci. Part B: Polym. Phys.* **1996**, *34*, 1213.
(35) Zhang, G. Ph.D. Thesis, University of Massachusetts: Amherst, 1994.
(36) Smith, D. B.; Johnson, K. S. *Gene* **1988**, *67*, 31.
(37) Le Grice, S. F. J.; Grueninger-Leitch, F. *Eur. J. Biochem.* **1990**, *187*, 307.
(38) Bujard, H.; Gentz, R.; Lanzer, M.; Stueber, D.; Mueller, M.; Ibrahimi, I.; Haeuptle, M.-T.; Dobberstein, B. *Methods Enzymol.* **1987**, *155*, 416.
(39) Mawn, M.; Tirrell, D. A.; Mason, T. L. Manuscript in preparation.

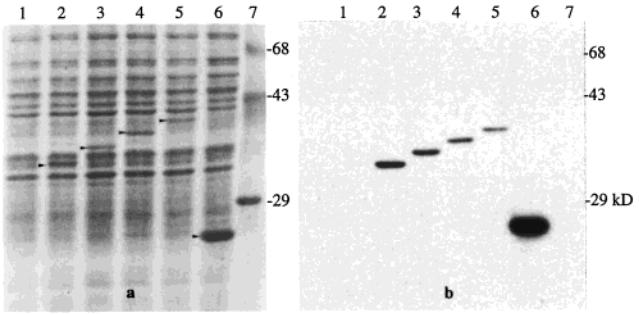

Figure 2. SDS-PAGE (12%) (a) and western blot (b) analyses of proteins in whole cell lysates. Lane 1 contains the nascent polypeptides derived from cells transformed with pQE15-3 before induction of target protein expression. Lanes 2 to 6 contain the nascent polypeptides derived from cells transformed with pQE15-*X* with $X = 3, 4, 5, 6$, and with pQE15, respectively, 3 h after target protein production had been initiated. Lane 7 contains molecular weight markers. The target protein bands are marked with arrowheads.

with IPTG (lane 1) but are present 3 h after protein synthesis is initiated. Expression of DHFR alone without multimeric insert is shown in lane 6. The intensities of the fusion protein bands (lanes 2−5) are significantly weaker than that of DHFR (lane 6), suggesting lower yields of the fusion proteins compared to DHFR alone. In addition, there is a marked decrease in the intensity of the protein bands as the length of the target protein increases (Figure 2b, lanes 2−5). This suggests that the yield of recombinant protein depends on the number of repeats appended to the fusion partner, decreasing as the number of repeats increases. The reasons for the low accumulation of the fusion protein and the decrease in protein yield with increasing chain length are not readily apparent; however, preliminary results suggest that plasmid instability, degradation of expressed protein, and inefficient transcription of the target gene sequence can be discounted.[40] The factors that control protein yield in this system are under active investigation.

Large-Scale Protein Expression and Purification. Expression of PLGA-*X* was scaled up to 60 L under conditions similar to those of the small scale experiments discussed above. Isolation of fusion proteins was accomplished under denaturing conditions by immobilized metal affinity chromatography.[37] The amount of isolated fusion protein decreased from approximately 10 mg/L to 5 mg/L as the length of the PLGA segment was increased from PLGA-3 to PLGA-6 (Table 1). In each case, PLGA-*X* was released from the fusion protein by cyanogen bromide cleavage and purified by anion-exchange chromatography. MALDI-TOF mass spectra of purified samples of PLGA-*X* are shown in Figure 3a; a spectrum of a conventional polydisperse PLGA (DP ≈ 8, PDI = 1.2) is presented in Figure 3b for comparison. The difference in polydispersity is striking; each biologically derived PLGA-*X* essentially shows only one signal, in contrast to the many signals (multiples of the repeating unit mass of 129 D) that appear in the spectrum of the conventional sample.[41]

Synthesis of PBLG-*X* (1). Benzylation of each PLGA-*X* was achieved by treating the acid form of the polymer with phenyldiazomethane. Preparation of the pure acid form of PLGA-*X* was found to be crucial for successful benzylation. Since the target protein is purified as the sodium salt, the protein has to be acidified prior to benzylation. During the acidification procedure, protein precipitated near pH 3, then redissolved as the pH was reduced to 1.4. In the pH 1.4 solution, protein eventually precipitated after overnight storage at 4 °C or during subsequent ultrafiltration. With PLGA-*X* isolated from pH 3 solution, the final yields of the side-chain alkylation were below 40%. The low yield is likely to be a consequence of incomplete acidification of the side chains. On the other hand, proteins isolated from pH 1.4 solutions gave more than 95% side-chain benzylation. Removal of residual salts from the protein was also essential for efficient benzylation of the side chains of PLGA-*X*. Ultrafiltration was performed on the acidified samples to remove residual salt and this procedure increased the side-chain benzylation yield from 65% to more than 95%. The proton NMR spectra of PBLG-3, -4, -5, and -6 are virtually identical with that of conventional PBLG with the exception of two weak benzyl aspartate resonances at 2.9 and 4.9 ppm.[26] Integration of the spectra indicated 94%, 98%, 95%, and 97% benzylation of the side chains of PLGA-3, -4, -5, and -6, respectively.

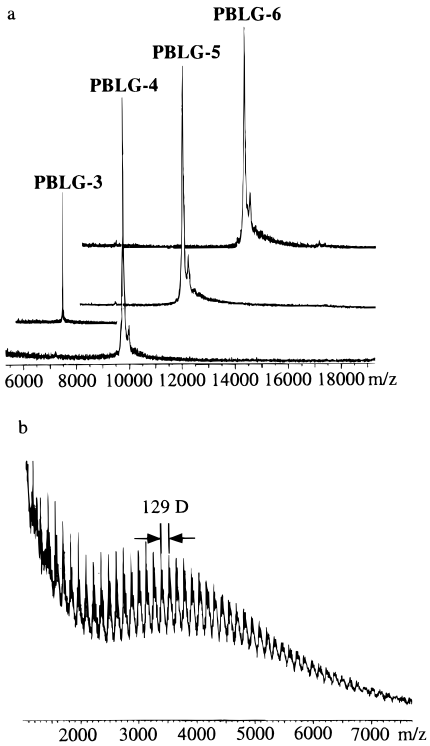

Figure 3. MALDI-TOF mass spectra of PLGA-*X* (a) and polydisperse PLGA (DP ≈ 92, PDI = 1.2) (b). Satellite signals that appear as high molecular weight shoulders in part a are due to a matrix−protein conjugate. The mass difference (129) between the major peaks in part b corresponds to the mass of the PLGA repeating unit. The finer scale splittings are due to sodium ion. Signals were collected in reflectance mode using sinapinic acid as the matrix.

Liquid Crystalline Phases of PBLG-*X* (1). PBLG liquid crystals are prepared simply by dissolving the polymer above its critical concentration in a solvent that supports the α-helical conformation. The formation of the liquid crystalline phase has been shown to proceed in stages as the concentration of polymer is increased.[42] When the PBLG concentration exceeds a certain minimum value, the solution separates into two phases. The PBLG-rich phase is birefringent and separates from the more dilute isotropic solution in the form of spherical liquid droplets. If the two-phase solution is cooled or the PBLG concentration

(40) Conticello, V. P.; Fournier, M. J.; Mason, T. L.; Tirrell, D. A. Manuscript in preparation.

(41) Shorter chains are detected preferentially in the MALDI-TOF mass spectrum of polydisperse PBLG. We suspect that longer chains are not detected because of aggregation which inhibits desorption of PBLG from the matrix.

(42) Du Pre, D. B.; Samulski, E. T. In *Liquid Crystals. The Fourth State of Matter*; Saeva, F. D., Ed.; Marcel Dekker: New York, 1979; p 203.

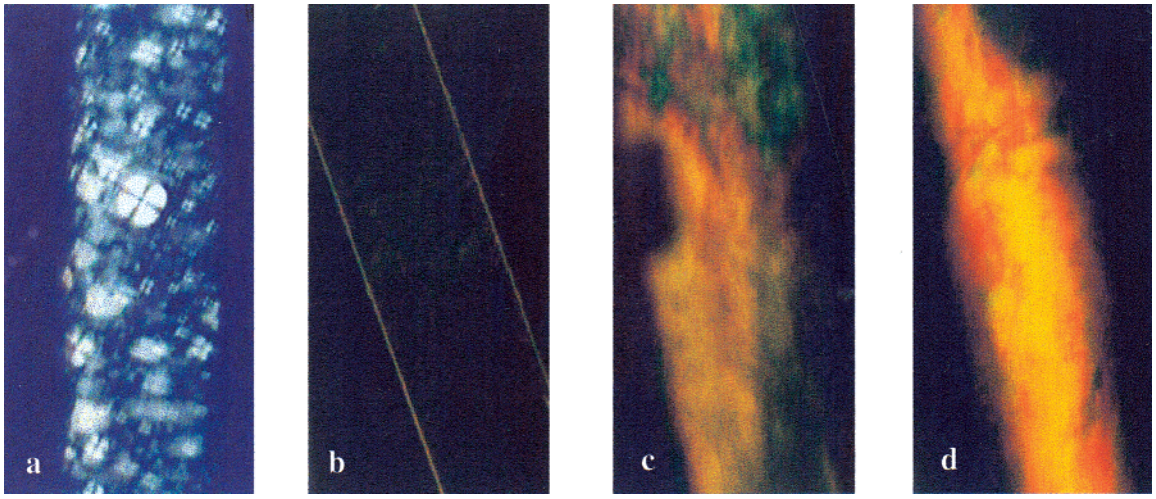

Figure 4. Polarized light optical micrographs of polydisperse PBLG (DP ≈ 98, PDI = 1.2, 22% w/v) (a) and PBLG-4 (22%, b; 33%, c; 45%, d) in solutions of $CHCl_3$(97%)/TFA(3%) in capillary tubes. In the polydisperse sample (a), a birefringent liquid crystalline phase separates in the form of spherical droplets (magnification ×20). In PBLG-4 (b−d), the phase transition occurs uniformly throughout the sample without formation of birefringent droplets (magnification ×40).

is increased further, the droplets grow in size and coalesce to form a continuous birefringent fluid. These reported results were reproducible when polydisperse PBLG (DP ≈ 98, PDI = 1.2) was investigated in mixtures of $CHCl_3$ (97%) and trifluoroacetic acid (TFA, 3%). PBLG has a strong tendency to aggregate in concentrated solutions and addition of TFA was reported to inhibit such aggregation while maintaining the rodlike conformation of the polymer.[43] Figure 4a shows the phase-separated birefringent droplets characteristic of a solution of approximately 22% of conventional PBLG (DP ≈ 98, PDI = 1.2) in $CHCl_3$-(97%)/TFA(3%). At higher concentrations, a typical fingerprint texture characteristic of the cholesteric phase was observed (data not shown). However, when solutions of monodisperse samples of PBLG-*X* were analyzed, different phase transition behavior was observed. First, PBLG-3 did not exhibit an anisotropic LC phase, even when concentration was increased to 40%. The longer polymers, PBLG-4, -5, and -6, on the other hand, all exhibited LC phases at high polymer concentrations. Because of our limited sample sizes, we did not determine precisely the concentration required for appearance of anisotropy for each of the monodisperse PBLG-*X*s. Determination of onset of anisotropy was complicated further by the fact that for the monodisperse polymers the initial appearance of a birefringent phase was not accompanied by formation of phase-separated birefringent droplets. The transition from the isotropic phase (Figure 4b) to the LC phase seemed to occur uniformly throughout the sample without the formation of clear phase boundaries as can be seen from the weakly birefringent sample of PBLG-4 in Figure 4c. When the concentration of this sample was increased further, the birefringent region became larger and brighter, and eventually filled the field of view (Figure 4d). This result suggests that the appearance of birefringent droplets in conventional PBLG may be a result of the polydisperse nature of PBLG prepared by chemical synthesis.

When analyzed as a thin film on a slide glass, the concentrated solutions (approximately 40%) of PBLG-4, -5, and -6 are highly birefringent and iridescent (Figure 5b−d); however, PBLG-3 (Figure 5a) appears dark. The aspect ratios of these polymers are listed in Table 2. The approximate aspect ratio of PBLG-3 is 6.9, which may be too small to allow formation of a stable LC phase. According to Flory's rod-ordering theory, the minimum aspect ratio for formation of a nematic liquid crystalline phase in neat liquid is 6.42.[44] Solutions of PBLG-4 and -5 occasionally yielded fanlike textures suggestive of smectic-like order; however, this texture was rarely seen in the PBLG-6 sample.[45] X-ray diffraction studies of concentrated PBLG samples in $CHCl_3$/TFA were precluded by strong scattering from the electron-rich $CHCl_3$ solvent. To prepare samples for diffraction, solvent-free films were prepared. When the solvent was evaporated from the concentrated samples, the

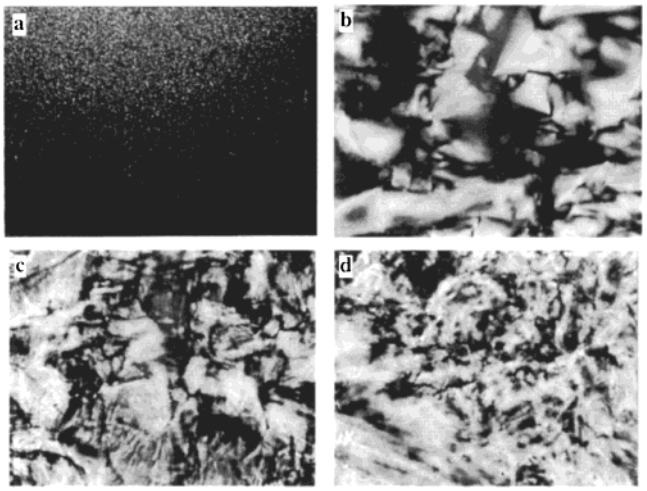

Figure 5. Polarized light optical micrographs of approximately 40% (w/v) solutions of PBLG-3 (a), PBLG-4 (b), PBLG-5 (c), and PBLG-6 (d) in $CHCl_3$(97%)/TFA(3%) (magnification ×200).

Table 2. Comparison of LC Properties of PBLG-*X* (**1**)

	PBLG-3	PBLG-4	PBLG-5	PBLG-6
no. of repeating units	58	76	94	112
rod length[a] (1.5 Å/repeat)	87 Å	114 Å	141 Å	168 Å
aspect ratio (L/D)[b]	6.9	9.1	11.3	13.4
order in concd solution	isotropic	smectic	smectic	unknown
obsd layer spacing[c]		114	140	

[a] In Å. [b] D = 12.5 Å (from ref 26). [c] In Å. From small-angle X-ray diffraction.

(43) Duke, R. W.; Du Pre, D. B.; Hines, W. A.; Samulski, E. T. *J. Am. Chem. Soc.* **1976**, *98*, 3094.

(44) Flory, P. J. *Adv. Polym. Sci.* **1984**, *59*, 1.

(45) Demus, D.; Richter, L. *Textures of Liquid Crystals*; Chemie: Weinheim, 1978.

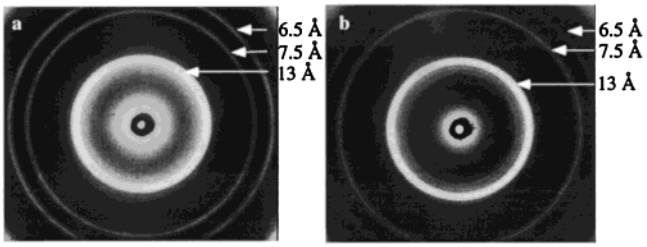

Figure 6. X-ray diffraction patterns of polydisperse PBLG (MW 20 100, PDI = 1.2) (a) and PBLG-4 (b) films cast from dioxane solutions.

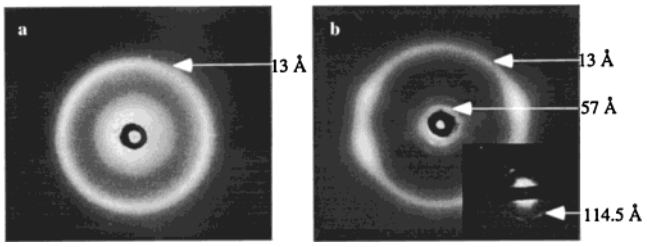

Figure 7. X-ray diffraction patterns of polydisperse PBLG (MW 20 100, PDI = 1.2) (a) and PBLG-4 (b) films cast from $CHCl_3$(97%)/TFA(3%) solutions. The inset in part b is a small-angle X-ray diffraction pattern of PBLG-4.

mesomorphic textures were retained, suggesting retention of LC organization during the drying process.

Smectic Ordering of PBLG-*X* (1) Films. For X-ray diffraction experiments, films of PBLG-*X* and polydisperse PBLG (DP ≈ 98, PDI = 1.2) were cast on Teflon plates. Concentrated solutions of PBLG in dioxane or $CHCl_3$(97%)/TFA (3%) were placed on Teflon plates and annealed by allowing the swollen films to remain in contact with solvent vapor for 4 days. After slow evaporation of the solvent, the films were dried in a vacuum for 2 days. Solution-cast films of PBLG have been reported to maintain their LC order after solvent evaporation, with molecular chains oriented parallel to the film surface.[46] X-ray diffraction patterns with the beam direction parallel to the surface of PBLG films indeed showed preferential orientation of PBLG rods parallel to the film surfaces (data not shown). Figure 6 shows wide-angle X-ray diffraction patterns (beam direction normal to the film surface) obtained from films of polydispserse PBLG (a) and from PBLG-4 (b) cast from dioxane solution. Both diffraction patterns show Bragg reflections at around 13 (very strong), 7.5 (strong), and 6.5 Å (strong). The 13 Å spacing is close to the reported value of the interchain distance of PBLG rods[10] and the ratios $(1:1/3^{1/2}:1/2)$ of spacings of the additional reflections suggest that the PBLG rods are packed in well-defined hexagonal order. The 13, 7.5, and 6.5 Å reflections can be assigned to the spacings of the (10), (11), and (20) lattice planes, respectively, of a 2-dimensional hexagonal lattice. No Bragg reflections were detected in the small-angle region for either of these films. Films of PBLG-5 and -6 yielded diffraction patterns almost identical to that of PBLG-4. These results indicate that films cast from dioxane solutions adopt columnar order, and that the ordering behavior does not depend on polydispersity.

Figure 7 compares the wide-angle X-ray diffraction patterns of polydisperse PBLG (a) and PBLG-4 (b) films cast from $CHCl_3$(97%)/TFA(3%) solutions. Both patterns are characterized by a diffuse wide-angle Bragg reflection with a spacing of 13 Å. The additional reflections which were present in the dioxane-cast films are not observed. Such diffraction patterns were typical of all $CHCl_3$/TFA-cast PBLG films. In $CHCl_3$/TFA solution-cast films, the PBLG rods are not packed with hexagonal order but are arranged with lateral disorder. In the polydisperse PBLG film, no other reflections were present in the diffraction pattern. However, in the diffraction pattern of the PBLG-4 film, additional reflections with Bragg spacings of 57 and 38 Å can been seen close to the beam stop.[47] The small-angle X-ray diffraction pattern (Figure 7b, inset) indicates a well-defined reflection at a spacing of 114.5 Å as well as the corresponding second-order reflection at 57 Å. A spacing of 114.5 Å is almost identical to the expected length of the PBLG helix, given the axial rise per residue of 1.5 Å of the α-helix and the degree of polymerization of 76. Densitometer scans of the small-angle X-ray diffraction patterns of monodisperse PBLG-*X* films cast from $CHCl_3$/TFA are presented in Figure 8. The PBLG-5 film shows a well-defined maximum at a spacing of 140 Å as well as the corresponding second-order reflection at 70 Å (trace b); these spacings are again commensurate with the length of the PBLG-5 helix (141 Å). The coincidence of the helix lengths and the observed layer spacings indicates smectic-like ordering in films of PBLG-4 and -5 cast from $CHCl_3$/TFA. However, films of PBLG-6 prepared in the same fashion did not show small-angle Bragg reflections (trace c). It is possible that the low mobility of PBLG-6 caused by its longer chain length may have slowed the ordering process.

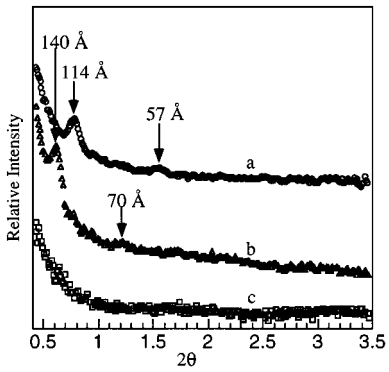

Figure 8. Densitometer scans of the small-angle X-ray diffraction patterns of films prepared from $CHCl_3$(97%)/TFA(3%) solutions of PBLG-4 (a), PBLG-5 (b), and PBLG-6 (c). The well-defined diffraction maxima with spacings of 114 and 140 Å are commensurate with the helix lengths of PBLG-4 and PBLG-5, respectively.

We speculate that the different ordering behavior of PBLG cast from dioxane and from $CHCl_3$/TFA is due to aggregation of the PBLG rods. It has been reported that PBLG has a strong tendency to aggregate even in dilute solutions.[48] The nature of the aggregation remains to be elucidated but such aggregation is reduced in polar solvents such as DMF and *m*-cresol.[49] Addition of a small amount of acid such as TFA or dichloroacetic acid is reported to disrupt the aggregation.[43] The columnar order in dioxane solutions suggests that in this solution the PBLG rods are aggregated predominantly in end-to-end fashion during or even before LC phase formation, which prevents smectic ordering. Once aggregation is disrupted by TFA, as in the PBLG-4 and -5 solutions in $CHCl_3$/TFA, the PBLG rods organize into the thermodynamically stable smectic phase, with

(46) Samulski, E. T.; Tobolsky, A. V. *Nature* **1967**, *216*, 997.

(47) The inhomogeneous azimuthal intensity distribution of the diffraction rings suggests that the PBLG-4 film is partially oriented. The Teflon plate used to cast this film contained scattered scratch marks which may have contributed to the orientation of the film. When films were cast on smooth surfaces these signals were observed as homogeneous rings.

(48) Powers, J. C. J.; Peticolas, W. L. *Advances in Chemistry*; American Chemical Society: Washington, DC, 1967; Vol. 63.

(49) Doty, P.; Bradbury, J. H.; Holtzer, A. M. *J. Am. Chem. Soc.* **1956**, *78*, 947.

the smectic layer spacing controlled precisely by the molecular chain length.

Conclusions

We have prepared a set of monodisperse rodlike artificial proteins PBLG-*X*, which vary in length from 8.7 to 17 nm. PBLG-3, with lowest aspect ratio (6.9), did not show evidence of LC behavior while the others showed lyotropic LC phases.

Solution-cast films of PBLG-4 and -5 form smectic-like supramolecular architectures with nanometer-scale layer spacings precisely controlled by the length of the monodisperse rods. Smectic order was observed only when samples were prepared from a nonaggregating solvent, a mixture of chloroform (97%) and trifluoroacetic acid (3%). In films cast from pure dioxane, both polydisperse and monodisperse PBLGs adopted columnar order without formation of smectic layers.

There have been many attempts to prepare well-ordered mono- and multilayers of PBLG at interfaces of various kinds. Ordered monolayers with rods oriented perpendicular to the substrate have been proposed as nonlinear optical and piezoelectric materials,[11−14] and mono- or multilayer films with rods organized parallel to the substrate may prove useful in creating patterned arrays for use in sensor technology.[15,50,51] However, highly ordered ultrathin PBLG films with well-defined architectures have not yet been achieved, perhaps because of the heterogeneous nature of conventional PBLGs. The synthetic methods described here, in which artificial genes encoding the polymers of interest are expressed in bacterial hosts, provide access to designed macromolecules with unprecedented control of molecular architecture. The monodisperse PBLG derivatives reported here may be expected not only to promote understanding of the fundamental physics of rodlike polymers, but also to have substantial impact in the application of rodlike polymers in a variety of technologies.

Acknowledgment. This work was supported by the National Science Foundation Materials Research Science and Engineering Center at the University of Massachusetts, and by grants from the Polymers and Genetics Programs of the NSF.

JA000465P

(50) Fukuto, M.; Heilmann, R. K.; Pershan, P. S.; Griffiths, J. A.; Yu, S. M.; Tirrell, D. A. *Phys. Rev. Lett.* **1998**, *81*, 3455.

(51) Fukuto, M.; Heilmann, R. K.; Pershan, P. S.; Yu, S. M.; Griffiths, J. A.; Tirrell, D. A. *J. Chem. Phys.* **1999**, *111*, 9761.